Quality Assurance and Safety of Crops & Foods, June 2014; 6 (2): 191-199

Wageningen Academic Publishers

Feasibility investigation of using artificial neural network in process monitoring of pumpkin air drying

M. Mokhtarian[1,2], F. Koushki[2], H. Bakhshabadi[3], B. Askari[2], A. Daraei Garmakhany[4] and S.H. Rashidzadeh[5]

[1]Islamic Azad University, Young Researchers Club, Sabzevar Branch, Sabzevar, Iran; [2]Islamic Azad University, Department of Food Science and Technology, Sabzevar Branch, Sabzevar, Iran; [3]Gorgan University of Agricultural Sciences and Natural Resources, Department of Food Science and Technology, Gorgan, Iran; [4]Bu-Ali Sina University, Toyserkan Faculty of Industrial Engineering, Department of Food Science and Technology, Hamadan, Iran; [5]Islamic Azad University, Young Researchers Club, Amol Branch, Amol, Iran; amirdaraey@yahoo.com

Received: 20 January 2012/ Accepted: 21 November 2012

RESEARCH ARTICLE

Abstract

In this paper, pumpkin cubes were dried by a laboratory scale convective hot air dryer. The drying process was carried out at four different temperatures (65, 75, 85 and 95 °C). After the end of drying process, initially, the experimental drying data were fitted with three well-known drying models. The results indicated that Newton model gave better results compared with other models to monitor the moisture ratio (MR) (with average correlation coefficient of determination, R^2=0.993). Also, this study used artificial neural network analysis (ANN) in order to feasibly predict dried pumpkins MR based on the time and temperature drying inputs. In order to do this project, two main activation functions including logsig and tanh that widely used in engineering calculations, were applied. Results showed that logsig activation function with 18 neurons in first hidden layer was selected as the best topology to predict MR. Comparison of the results obtained by ANN and classical modelling showed that artificial neural approach has a higher ability compared to classical modelling in predicting MR (R^2=0.9991 and 0.993, respectively).

Keywords: empirical modelling, perceptron neural network, thin-layer drying

1. Introduction

Pumpkin is a seasonal crop that has been used traditionally. It covers a wide range of species of the *Cucurbitaceae* family of which many have potential economic value (Terazowa *et al.*, 2001). Since pumpkin is available only seasonally, drying techniques can be used to preserve it. Many studies have been conducted in field of pumpkin drying. For instance, De Souza Silva *et al.* (2011) investigated the effect of osmotic dehydration for low temperature blanched pumpkin. The results revealed that blanching changed the pumpkin colour, whereas osmotic dehydration did not change it significantly. The impregnation process maintained or even increased the tissue firmness compared to the blanching method.

Furthermore, Mayor *et al.* (2011) studied the physical properties variation of pumpkin undergoing osmotic dehydration. They mentioned that pumpkin shrinkage was isotropic. Moreover, Guine *et al.* (2010) worked on pumpkin drying behaviour. Their results illustrated that increase of drying temperature could strongly accelerate the drying process, so that the process was taken at 30 °C for 8 h while the drying was finished at 70 °C after just 2 h. The experimental data were fitted to different models for moisture ratio (MR) prediction and they concluded that the best models were Page and modified Page.

Afterward, Shafafi Zenoozian *et al.* (2008) studied the effect of osmotic dehydration as a pre-treatment on hot-air drying kinetics of pumpkin to evaluate the most excellent model for hot-air drying of pumpkin. They also apply a computer vision system to monitor the colour changes during drying. Results showed that two-term equation had best performance for modelling sucrose preosmosed samples, whereas the modified Henderson and Pabis model represented tremendous harmonious with samples treated through the sorbitol solution.

Sacilik (2007) studied the effect of drying methods on thin-layer drying characteristics of hull-less seed pumpkin (*Cucurbita pepo* L.). He explained that the logarithmic model had the best fit to experimental data with correlation coefficient (R^2) greater than 0.99 for hot air and solar tunnel drying process.

Recently, neural networks have been enforced as influential tool for estimating the food properties variation during drying process. Several studies have been done in the field of food modelling by use of artificial neural networks (ANN). Tavakolipour and Mokhtarian (2012) applied the ANN approach to predict moisture ratio of dried pistachio nuts. Their results showed that the perceptron neural network with 7 neurons in the first and second hidden layer was able to predict the moisture ratio with R^2=0.994. Aghajani *et al.* (2012), Kashiri *et al.* (2012) and Shahabi Ghahfarrokhi *et al.* (2013) used ANN in their study to evaluate the drying process of green malt, modeling of sorghum soaking and estimation of peroxidase enzyme activity in vegetables, respectively. In addition, Shafafi Zenoozian and Devahastin (2009) studied dehydration behaviour of pumpkin during drying process by use of wavelet transform coupled with ANN to predict the food properties. This research exhibited that wavelet coefficients obtained by decomposition of pumpkin images could be utilised as input variables for constructing ANN models to estimate some physicochemical changes of osmotically dehydrated pumpkin. The best models could predict MR, Heywood shape factor and colour change with R^2>0.9957 in all cases, except when pumpkin was osmotically dehydrated by glucose solution, with R^2=0.9102 when predicting MR. Besides, Menlik *et al.* (2010) explained freeze-drying behaviour of apple by ANN. They used back-propagation with learning algorithm of Levenberg-Marquardt and Fermi transfer function in their study.

The aim of this research was to predict drying kinetics of pumpkin by mathematical models and select the best model among three thin layer drying models and also develop a neural network model using multilayer perception (MLP) architecture for MR estimation of dried pumpkin.

2. Materials and methods

Raw material preparation

Pumpkin (*Cucurbita mixta*) were purchased from a local market and stored at 5 °C until the experiment. At the beginning of each experiment, pumpkin was washed and cut into pieces with dimensions of (20×20×5 mm). The initial moisture content of samples was determined by hot oven (Memmert, model UNE 400 PA; Scheabach, Germany) at 105 °C for 48 h according to AOAC method 931.04 (AOAC, 1990). Average initial moisture content of pumpkin was found to be 11.67±0.5 (% dry basis).

Drying equipment

A laboratory convective hot-air dryer (model Of-02G; JEIO TECH, Seoul, Korea) was applied in the experiment. The experiment was carried out at four temperatures 65, 75, 85 and 95 °C. The relative humidity of the ambient air (~30 °C) was around 62-65%. The dryer was adjusted to a congenial temperature and became constant for 1.5 h before the experiment. When the fan motor switch was turned on, inlet air would distribute inside the chamber and then passed through a hot oven. The weight loss was monitored by means of a digital balance (FX-300 CT; A&D Co., Ltd, Tokyo, Japan) by sampling interval of 30 min during the drying process. The final weight and moisture content of the pumpkin pieces were measured at the end of each drying experiment. Drying was finished when the moisture content of the samples reached to 0.15±0.5 (% dry basis).

Mathematical modelling of drying process

Thin-layer drying models for experimental data of pumpkin cubes were expressed in the form of MR of samples during thin-layer drying and it was displayed as Equation 1:

$$MR = \frac{M - M_e}{M_0 - M_e} \quad (1)$$

Also, the drying rate (DR) of pumpkin cubes under drying can be computed by Equation 2:

$$DR = \frac{M_{t+dt} - M_t}{dt} \quad (2)$$

In these equations, M, M_0, M_e, M_t and M_{t+dt} are the moisture content at any time, initial moisture content, equilibrium moisture content, moisture content at time t and moisture content at time t+dt (kg water/kg dry matter), respectively, t is drying time (min). Drying experiments were done in three replications. Functions and mathematical models were simulated by SigmaPlot, version 11 (London, UK). The drying curves obtained were fitted with three different MR models (Table 1) (Togrül and Pehlivan, 2002).

R^2 was one of the main criteria for selecting the best equation. In addition to R^2, the goodness of fit was determined by various statistical parameters such as reduced chi square (χ^2), mean relative deviation modulus P(%) and root mean square error (RMSE). For quality fit, R^2 value should be higher and χ^2, P(%) and RMSE values should be lower (Goyal *et al.*, 2008). The above parameters can be calculated as follows:

Table 1. Drying kinetic models.

Equation	Model name
MR = exp(-kt)	Newton
MR = a exp(-kt)	Henderson and Pabis
MR = a exp(-c(t/L^2))	Diffusion

A, c, L = model constants; k = kinetic constant (1/min); MR = moisture ratio; t = drying time (min).

$$\chi^2 = \frac{\sum_{i=1}^{N} (MR_{exp,i} - MR_{per,i})^2}{N - z} \tag{3}$$

$$P(\%) = \frac{100}{N} \sum_{i=1}^{N} |MR_{per,i} - MR_{exp,i}| \tag{4}$$

$$RMSE = [\frac{1}{N} \sum_{i=1}^{N} (MR_{per,i} - MR_{exp,i})]^{\frac{1}{2}} \tag{5}$$

Where $MR_{exp,i}$ is the experimental moisture ratio, $MR_{per,i}$ is the predicted moisture ratio, N is the number of experimental data and z is the number of model parameters.

Computation of effective diffusion coefficient and activation energy

The experimental drying data were used for determination of diffusivity coefficients by Fick's second diffusion equation. The analytical solution of Fick's second law is unsteady state diffusion in an infinite slab by the drying process is shown in Equation 6 (Van Arsdel and Copley, 1963):

$$MR = \frac{M - M_e}{M_0 - M_e} = \frac{8}{\pi^2} \exp\left[\frac{-\pi^2 D_{eff} t}{4L^2}\right] \tag{6}$$

Where D_{eff} is the effective diffusion coefficient (m^2/s) and L is the half-thickness of a sample (m). Therefore, D_{eff} was obtained by plotting ln(MR) versus time (min). From Equation 6, a plot of ln(MR) versus time displayed a straight line with a slope of α:

$$\alpha = \frac{\pi^2 D_{eff}}{4L^2} \tag{7}$$

The temperature dependence of D_{eff} was expressed by the Arrhenius relationship:

$$D_{eff} = D_0 \exp\left(-\frac{E_a}{RT}\right) \tag{8}$$

Taking the logarithm of the above equation gives:

$$\ln(D_{eff}) = \ln(D_0) - \frac{E_a}{RT} \tag{9}$$

Where D_o is the pre-exponential constant (m^2/s), E_a is the activation energy (kJ/mol), R is the universal gas constant (kJ/mol K) and T is the temperature (K). When plotting $\ln(D_{eff})$ versus 1/T, the activation energy (E_a) and pre-exponential constant (D_o) can be obtained.

Artificial neural network

An ANN composed of simple processing elements called neurons that are connected to each other by weights. The neuron is grouped into distinct layers and interconnected according to a given architecture (Mousavi and Javan, 2009; Tavakolipour and Mokhtarian, 2012). MLP networks is one of the most popular and successful neural network architectures, suited to wide range of engineering application involved drying (Aghajani *et al.*, 2012; Kashiri *et al.*, 2012).Mathematically:

$$y_i = \sum_{i=1}^{n} f(w_{ij} x_i) + b_j \tag{10}$$

Where y_j is the net input of each neuron in hidden and output layers, x_i is the input, n is the number of inputs to the neuron, w_{ij} is the weight of the connection between neuron i and neuron j and b_j is the bias associated with the j^{th} neuron (Mohebbi *et al.*, 2010). Each neuron consists of a transfer function expressing its internal activation level. Output from a neuron is determined by transforming its input using a suitable transfer function.

Generally, the transfer functions are sigmoidal, Gaussian, hyperbolic tangent, hyperbolic secant and linear functions. The sigmoidal (logsig) and hyperbolic tangent (tanh) functions are used to establish a non-linear relationship in engineering applications (Picton, 2000):

$$\text{logsig}(z) = \frac{1}{1 + \exp(-z)} \quad (0, +1) \tag{11}$$

$$\tanh(z) = \frac{e^z - e^{-z}}{e^z + e^{-z}} \quad (-1, +1) \tag{12}$$

Figure 1 shows a schematic structure of a perceptron neural network. In this network, the input layer consists of two neurons (air temperature and drying time; x_1 and x_2, respectively)) and the output layer contains one neuron (moisture ratio; y).

The back propagation algorithm was used in training of ANN model. This algorithm uses the supervised training technique where the network weights and biases are initialised randomly at the beginning of the training phase (Singh and Pandey, 2011). In order to optimise ANN, different factors including hidden layer number, number of neuron per hidden layer, type of activation function in hidden and output layers, learning rate and momentum coefficients must be evaluated. In this work, number of 1-2 hidden layers with 2-23 neurons per hidden layer, learning rate = 0.4, momentum coefficient = 0.9 and activation functions of sigmoid logarithms (Equation 11) and hyperbolic tangent (Equation 12) in each hidden and output layer were used in order to find the best topology.

In order to model the network, the data were randomly divided into three groups, including 60% for training, 20%

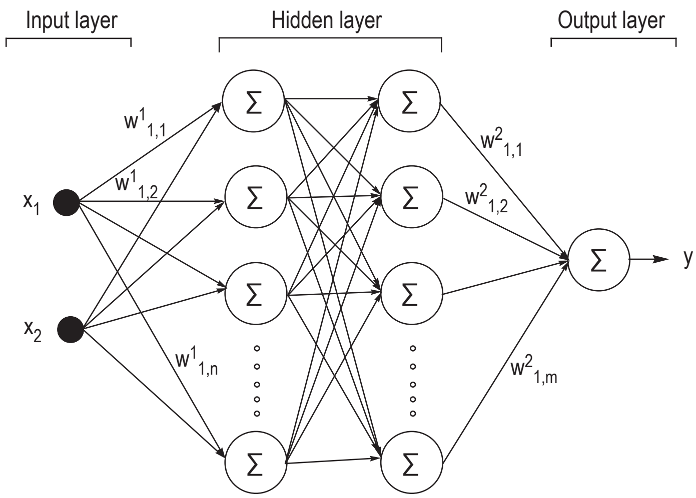

Figure 1. Schematic structure of a perceptron neural network.

for cross validation, and 20% for testing of the network. Data modelling was accomplished by using SPSS statistical software, version 19 (2011, Armonk, NY, USA). For determination of the best network arrangement, two criteria were used: the determination coefficient (R^2) and the mean relative error (MRE), which were calculated as follows:

$$R^2 = 1 - \left[\frac{\sum_{i=1}^{N}(MR_{ANN,i} - MR_{exp,i})^2}{\sum_{i=1}^{N}(\overline{MR}_{ANN,i} - MR_{ANN,i})^2} \right] \quad (13)$$

$$MRE = \left(\frac{1}{N} \sum_{i=1}^{N} \frac{|(MR_{ANN,i} - MR_{exp,i})|}{MR_{exp,i}} \right) \times 100 \quad (14)$$

Where MR_{ANN} is the predicted ANN output parameter, MR_{exp} is the experimental data and N is the number of observations.

3. Results and discussion

Drying kinetics of pumpkin

The three thin-layer drying models were evaluated in terms of the statistical parameters R^2, χ^2, P(%) and RMSE. The results of statistical analysis are shown in Table 2 for different temperatures. As can be seen, in all experiments, the R^2 values were greater than 0.9803. On the other hand, the Newton model displayed a lower P(%), χ^2 and RMSE values. Thus, based on the R^2 and P(%), χ^2 and RMSE values, it can be concluded that the Newton model represented the best results to illustrate the thin-layer drying characteristics of pumpkin cubes at 65, 75, 85 and 95 °C compared to other models.

Figure 2 exhibits the comparison between predicted and experimental data of thin-layer drying of pumpkin cubes at the temperatures of 65, 75, 85 and 95 °C for the Newton model. The model represented MR values banded along a straight line, which demonstrated the fitness of these models for describing the drying characteristics of pumpkin sample. Similar results have been reported by other researchers (Hassan-Beygi *et al.*, 2009; Menges and Ertekin, 2006).

Table 2. Results of statistical analyses on thin layer drying of pumpkin.

Model	T (°C)	R^2	χ^2	P(%)	RMSE
Newton	65	0.9965	0.00037	1.525	0.0757
	75	0.9837	0.00211	3.73	0.1013
	85	0.9936	0.00083	2.21	0.0889
	95	0.9988	0.00016	0.87	0.0620
Henderson and Pabis	65	0.9964	0.00037	1.533	0.0836
	75	0.9831	0.0022	3.80	0.1196
	85	0.9929	0.00092	2.31	0.0990
	95	0.9986	0.00019	0.91	0.0662
Diffusion	65	0.9961	0.00041	1.533	0.0836
	75	0.9803	0.00255	3.80	0.1197
	85	0.9915	0.00110	2.31	0.0990
	95	0.9983	0.00023	0.91	0.0662

P(%) = mean relative deviation modulus; R^2 = coefficient of determination; RMSE = root mean square error; T = drying temperature; χ^2 = chi square.

In addition, parameters of various applied models are presented in Table 3. The kinetic constant (k) increased as drying temperature increased thus it can be predicted by Arrhenius relationship (Equation 15). By taking logarithm from both side of Equation 15 and plot ln(k) versus 1/T, first order regression can fitted data with a high R^2 (0.9251) that are shown in Figure 3.

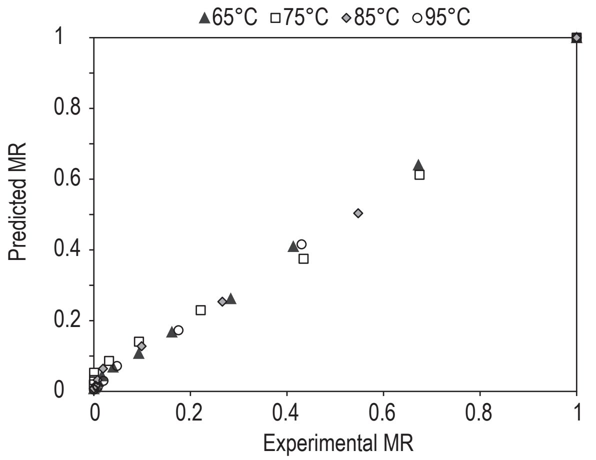

Figure 2. Correlation between experimental and predicted moisture ratio (MR) by Newton model during air drying.

Table 3. Parameters of applied models at different temperatures.

Model names	T (°C)	k (1/min)	a	c	L
Newton	65	0.0293	-	-	-
	75	0.0310	-	-	-
	85	0.0317	-	-	-
	95	0.0323	-	-	-
Henderson and Pabis	65	0.0151	1.017	-	-
	75	0.0168	1.036	-	-
	85	0.0232	1.016	-	-
	95	0.0293	1.004	-	-
Diffusion	65	-	1.53	1.78	9.15
	75	-	3.09	2.71	8.32
	85	-	1.39	1.95	7.66
	95	-	1.08	1.72	7.22

A, c, L = model constants; k = kinetic constant; T = temperature.

$$k = k_0 \exp(\frac{E_a}{RT}) \quad (15)$$

The variation of MR versus drying time for pumpkin samples at different temperatures is shown in Figure 4. As can be seen, MR decreases recurrently by increase of drying time. As expected for these drying curves, the drying air temperature had much more effect on the MR of pumpkin cubes. On the other hand, an increase in drying air temperature lead to decrease of drying time. The drying time to reach the final moisture content of pumpkin cubes were 330, 240, 210 and 180 min at drying temperatures of 65, 75, 85 and 95 °C, respectively. Our results are in agreement with those found by Ramaswamy and Van Nieuwenhuijzen (2002) on drying of apple slices.

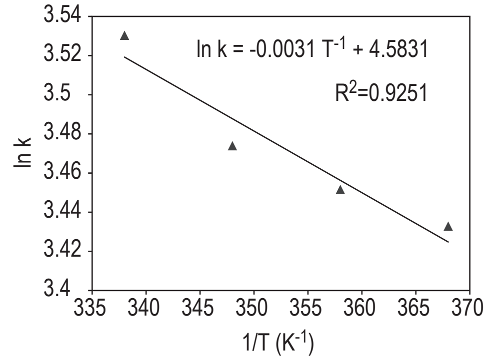

Figure 3. Arrhenius-type relationship between the logarithm of the kinetic parameter (k) of the Newton model versus inverse temperature (1/T).

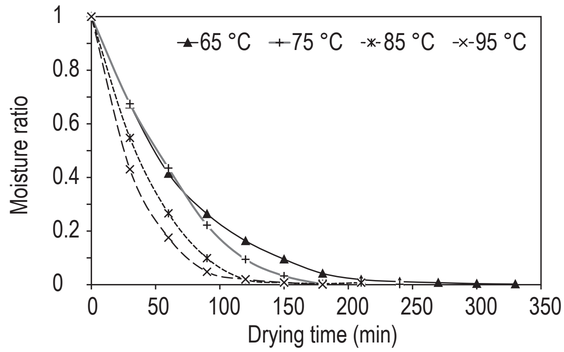

Figure 4. The variation of moisture ratio of pumpkin samples against drying time at different temperatures.

At a brief glance, it can be seen that increasing the air temperature lead to increase of drying rate. Figure 5 reveals the variation of drying rate versus time in the different temperature of thin-layer drying of pumpkin cubes. Similar results were published by Mwithiga and Ochieng Olwal (2005).

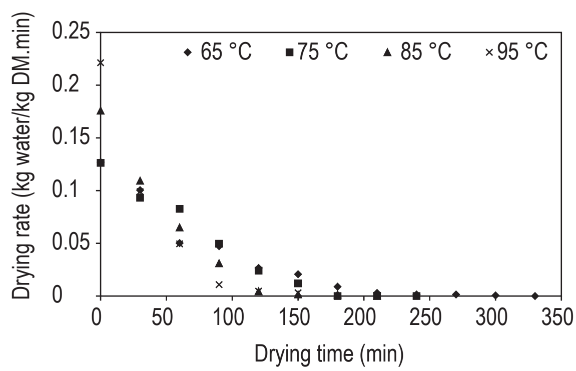

Figure 5. Variation of drying rate versus drying time at different temperatures.

The effective moisture diffusivity values of pumpkin samples are listed in Table 4 for different temperatures. It was found that effective moisture diffusion ranged from 1.5793×10^{-10} to 1.2829×10^{-9} m^2/s. Also, the moisture diffusivity showed the accelerating trend by increase of drying temperature. According to Table 4, it can be easily concluded that the effective moisture diffusivity values for dried samples at 95 °C were higher than dried samples at 65 °C. The D_{eff} values were given in Table 5 for pumpkin (present study) and other products.

The activation energy was computed through curving the $\ln(D_{eff})$ against the inverse of the temperature $(1/(T + 273.15))$, and represented in Figure 6.

The activation energy value was acquired to be 68.884 kJ/mol at present work. This value is greater than the activation energy of sweet cherry drying (43.05 and 49.17 kJ/mol for the control and pre-treated samples, respectively; Doymaz and Ismail, 2011), carrot drying (28.36 kJ/mol; Doymaz, 2004a) and tomato drying (17.4-32.94 kJ/mol; Doymaz, 2007).

Modelling of artificial neural approach

In this research, a combination of different layers and neurons with different activation functions were used for modelling Perceptron neural networks. Neural network with one and two hidden layers, 1 to 22 neurons were selected randomly and network power was estimated to predict pumpkin MR. To obtain suitable training epoch experimental network was used with variable numbers of neuron (1 to 22 neurons) and suitable training epoch number was determined for each activated function. In order to identify the best training epoch, trial and error method was used (Applied training epoch number were as follows: 100, 1000, 1,500, 2,500, 5,000 and 7,000). Achieving the lowest relative error ratio was the main issue for optimising the best training epoch in each activated function. The results showed that the best training epoch for logsig and tanh activation function were 7,000 and 5,000, respectively. The results of MLP were optimised with logsig and hyperbolic tanh activation function and topologies in different cases achieved as indicated by Figure 7 and 8. Figure 7 shows the variation of MRE values versus neuron numbers to predict MR. Investigating the obtained results for MLP with logsig activated function with one and two hidden layer has been shown, topologies 2-18-1 (i.e. network with 2 inputs, 18 neurons in the first hidden layer and one output) and 2-16-16-1 (i.e. network with 2 inputs, 16 neurons in the first and second hidden layer and one output) had the best result to predict MR. In this case, R^2 values were calculated to be 0.999 and 0.997, respectively. On the other hand, the results of MLP with tanh activation

Table 4. Effective diffusion coefficient (D_{eff}) for dried pumpkin at optimum conditions

T (°C)	D_{eff} (m^2/s)$\times 10^{-9}$ (m^2/s)	R^2
65	0.158	0.993
75	0.757	0.930
85	1.019	0.924
95	1.283	0.931

R^2 = coefficient of determination; T = air temperature.

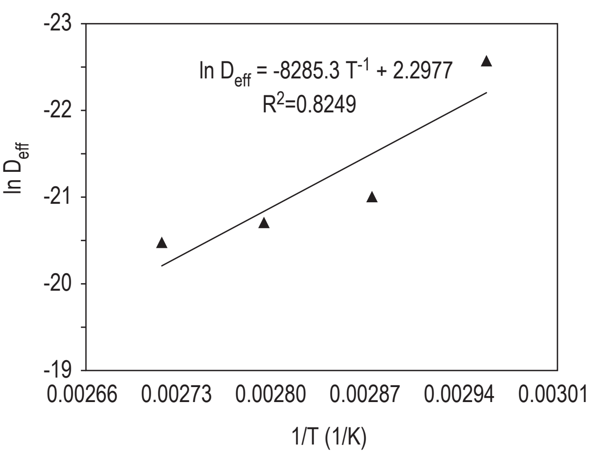

Figure 6. The logarithm of the effective diffusion coefficient (D_{eff}) versus the inverse of temperature (1/T).

Table 5. Effective diffusion coefficient (D_{eff}) of pumpkin fruit and other products.

Products	Temperature (°C)	D_{eff} (m^2/s)	Reference
Organic apple	40 - 60	$2.27 - 4.97 \times 10^{-10}$	Sacilik and Elicin (2006)
Apricot	55	$6.76 - 12.6 \times 10^{-10}$	Doymaz (2004b)
Sweet cherry	60 - 75	$1.54 - 5.68 \times 10^{-10}$	Doymaz and Ismail (2011)
Tomato	55 - 70	$3.91 - 6.65 \times 10^{-10}$	Doymaz (2007)
Carrot	50 - 70	$0.77 - 9.33 \times 10^{-9}$	Doymaz (2004a)
Pumpkin	65 - 95	$0.158 - 1.283 \times 10^{-9}$	Present study

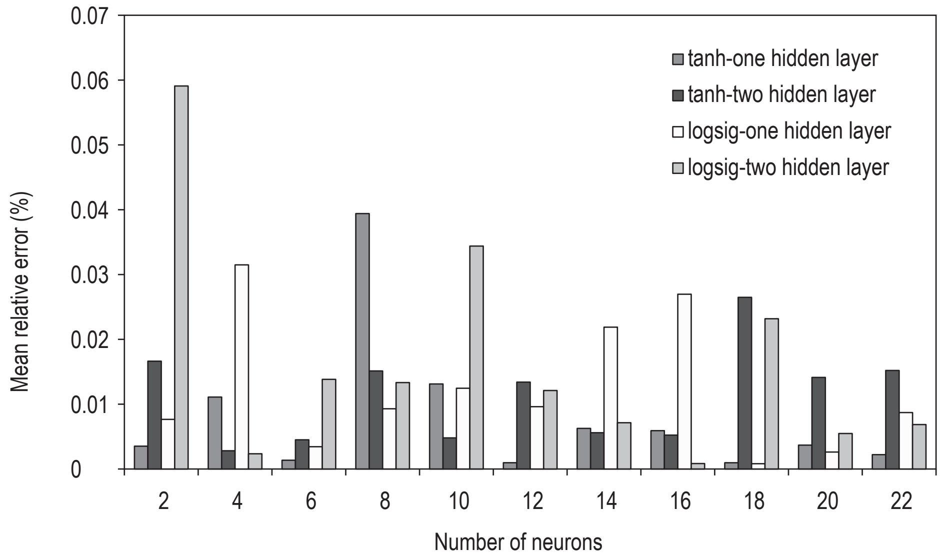

Figure 7. Variation of the relative error values versus neuron numbers to predict the moisture ratio with different activation function during drying.

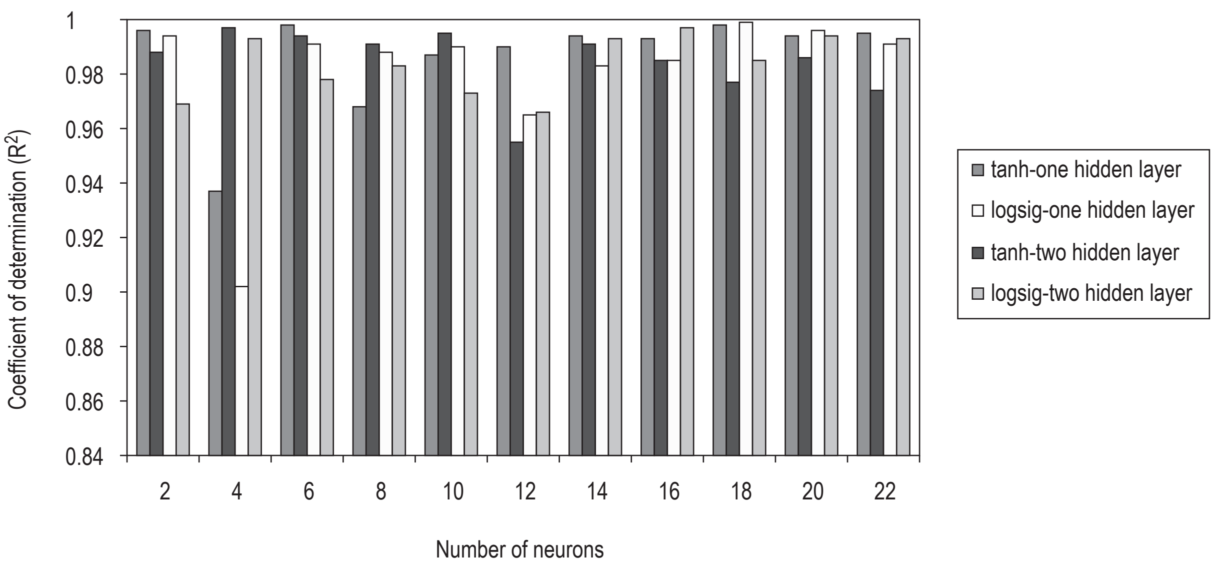

Figure 8. Variation of correlation coefficient (R^2) versus neuron numbers to predict the moisture ratio with different activation function during drying.

function showed that neural network with topology 2-18-1 had the best result to optimise MR; accordingly, this network could predict MR with R^2=0.998 (in this case, MRE was calculated to be 0.000966%). Similar results were reported by Tavakolipour and Mokhtarian (2012) in case of pistachio nuts.

The results of comparison ANN with different functions indicated that logsig function with 18 neurons in hidden layers was the best topology to predict MR of dried pumpkins. A model sensitivity diagram of predicted parameters by MLP network with logsig activation function versus experimental parameters for the best topology (i.e. structure of 2-18-1) indicated that data were randomly located around the regression line. This could be a reason for carefully evaluating the neural networks to predict MR of pumpkin during convective hot air drying (Figure 9).

4. Conclusions

In this research, ANN trained by back propagation algorithms was developed to feasibly predict MR based on the two input variables. Different factors including learning epochs (100 to 7,000), number of neurons (1 to 22) and type

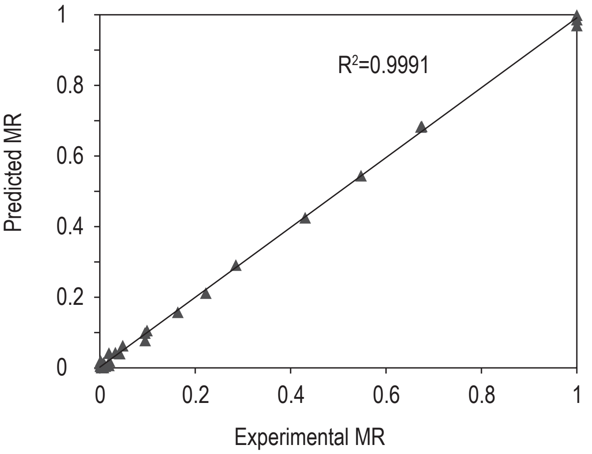

Figure 9. Comparison between experimental and predicted moisture ratio (MR) value obtained by goodness activation function of the artificial neural network (logsig).

of activation function in hidden and output layers (logsig and tanh) were used in order to find the best topology of ANN for monitoring MR during drying. The results indicate that, ANN with logsig activation function with 18 neurons in first hidden layer (i.e. 2-18-1 topology) was able to estimate MR with higher R^2 value (0.9991), whereas the Newton model (as the best model) could predict MR with average R^2=0.993. Overall the comparison of obtained results of ANN and empirical modelling showed that ANN (as a non-destructive method) had a higher ability than classical modelling to predict MR.

References

Aghajani, N., Kashaninejad, M., Dehghani, A.A. and Daraei Garmakhany, A., 2012. Comparison between artificial neural networks and mathematical models for moisture ratio estimation in two varieties of green malt. Quality Assurance and Safety of Crops and Foods 4: 93-101.

Association of Official Analytical Chemists (AOAC), 1990. AOAC official method 931.04. Moisture in cacao products. AOAC, Washington, DC, USA.

De Souza Silva, K., Cássia Caetano, L., Castilho Garcia, C., Telis Romero, J., Barbosa Santos, A., Aparecida Mauro, M. and Ismail, O., 2011. Osmotic dehydration process for low temperature blanched pumpkin. Journal of Food Engineering 105: 56-64.

Doymaz, I., 2004a. Convective air drying characteristics of thin layer carrots. Journal of Food Engineering 61: 359-364.

Doymaz, I., 2004b. Effect of pre-treatments using potassium metabisulphide and alkaline ethyl-oleate on the drying kinetics of apricots. Journal of Biosystems Engineering 89: 281-287.

Doymaz, I., 2007. Air-drying characteristics of tomatoes. Journal of Food Engineering 78: 1291-1297.

Doymaz, I. and Ismail, O., 2011. Drying characteristics of sweet cherry. Journal of Food and Bioproducts Processing 89: 31-38.

Goyal, R.K., Mujjeb, O. and Bhargava, V.K., 2008. Mathematical modeling of thin layer drying kinetics of apple in tunnel dryer. International Journal of Food Engineering 4: 1-16.

Guiné, R.P.F., Pinho, S. and Barroca, M.J., 2010. Study of the convective drying of pumpkin (*Cucurbita maxima*). Journal of Food and Bioproducts Processing 89: 422-428.

Hassan-Beygi, S.R., Aghbashlo, M., Kianmehr, M.H. and Massah, J., 2009. Drying characteristics of walnut (*Juglans regia* L.) during convection drying. Journal of International Agrophysics 23: 129-135.

Kashiri, M., Daraei Garmakhany, A. and Deghani, A.A., 2012. Modeling of Sorghum soaking using artificial neural networks (MLP). Quality Assurance and Safety of Crops and Foods 4: 179-184.

Mayor, L., Moreira, R. and Sereno, A.M., 2011. Shrinkage, density, porosity and shape changes during dehydration of pumpkin (*Cucurbita pepo* L.) fruits. Journal of Food Engineering 103: 29-37.

Menges, H.O. and Ertekin, C., 2006. Modeling of air drying of Hacihaliloglu-type apricots. Journal of the Science of Food and Agriculture 86: 279-291.

Menlik, T., Bahadır Özdemir, M. and Kirmaci, V., 2010. Determination of freeze-drying behaviors of apples by artificial neural network. Journal of Expert Systems with Applications 37: 7669-7677.

Mohebbi, M., Shahidi, F., Fathi, M., Ehtiati, A. and Noshad, M., 2010. Prediction of moisture content in pre-osmosed and ultrasounded dried banana using genetic algorithm and neural network. Food and Bioproduct Processing 89: 362-366.

Mousavi, M. and Javan, S., 2009. Modeling and simulation of apple drying, using artificial neural network and neuro-taguchi's method. Journal of Agricultural Science and Technology 11: 559-571.

Mwithiga, G. and Ochieng Olwal, J., 2005. The drying kinetics of kale (*Brassica oleracea*) in a convective hot air dryer. Journal of Food Engineering 71: 373-378.

Picton, P., 2000. Introduction to neural networks. Palgrave Macmillan, Basingstoke, UK, 176 pp.

Ramaswamy, H.S. and Van Nieuwenhuijzen, N.H., 2002. Evaluation and modeling of two-stage osmo-convective drying of apple slices. Journal of Drying Technology 20: 651-667.

Sacilik, K., 2007. Effect of drying methods on thin-layer drying characteristics of hull-less seed pumpkin (*Cucurbita pepo* L.). Journal of Food Engineering 79: 23-30.

Sacilik, K. and Elicin, A.K., 2006. The thin layer drying characteristics of organic apple slices. Journal of Food Engineering 73: 281-289.

Shahabi Ghahfarrokhi, I., Daraei Garmakhany, A., Kashaninejad, M. and Dehghani, A.A., 2013. Estimation of peroxidase activity in red cabbage by artificial neural network. Quality Assurance and Safety of Crops and Foods 5:163-167.

Shafafi Zenoozian, M. and Devahastin, S., 2009. Application of wavelet transform coupled with artificial neural network for predicting physicochemical properties of osmotically dehydrated pumpkin. Journal of Food Engineering 90: 219-227.

Shafafi Zenoozian, M., Devahastin, S., Razavi, S.M.A., Shahidi, F. and Pourreza, H.R., 2008. Image use of artificial neural network and image analysis to predict physical properties of osmotically dehydrated pumpkin. Journal of Drying Technology 32: 88-102.

Singh, N.J. and Pandey, R.K., 2011. Neural network approaches for prediction of drying kinetics during drying of sweet potato. Agricultural Engineering International: CIGR Journal 13: 1-7.

Tavakolipour, H. and Mokhtarian, M., 2012. Neural network approaches for prediction of pistachio drying kinetics. International Journal of Food Engineering 8: 42.

Terazowa, Y., Ito, K. and Yoshida, K., 2001. Changes in carbohydrate composition in pumpkin (kabocha) during fruit growth. Journal of the Japanese Society Horticultural Science 70: 656-658.

Togrül, I.T. and Pehlivan, D., 2002. Mathematical modelling of solar drying of apricots in thin layers. Journal of Food Engineering 55: 209-216.

Van Arsdel, N.B. and Copley, M.J., 1963. Food dehydration. AVI Publishing, Westpoint, CT, USA.